 https://doi.org/10.3311/PPci.18151

Periodica Polytechnica Civil Engineering, 66(1), pp. 228–234, 2022

Estimation of Rheological Effects in Cantilever Concrete Bridges on the Basis of a Span's Deflection Line

Bartosz Pisarek[1*], Czeslaw Machelski[2]

[1] Wayss & Freytag Ingenieurbau AG, Eschoborner Landstrasse 130-132, 60489 Frankfurt am Main, Germany
[2] Department of Bridge and Raailway, Wroclaw University of Science and Technology, Wybrzeże Stanisława Wyspiańskiego 41 (27*) budynek H-3, PWr, 50-370 Wroclaw, Poland
[*] Corresponding author, e-mail: bartosz.pisarek@wf.bam.com

Received: 07 March 2021, Accepted: 23 September 2021, Published online: 15 November 2021

Abstract

A characteristic feature of bridges as large span objects made using cantilever concreting technology are their excessive deflections, which are a result of rheological processes in concrete and pre-stressing steel. These deflections can be caused by the destruction of the material, e.g., concrete cracking, as well as the changing of the static scheme of the bridge structure, such as the subsidence of supports. The purpose of the work is to determine internal forces based on the deformation of a span. An algorithm for the correction of the deflection function, which is determined from geodetic measurements with a low accuracy, was proposed. It is characterized by a marked improvement in the results of calculations and, to a small extent, leads to the smoothing of the original measurement results. The algorithm is adapted to the analysis of a selected fragment of the structure, e.g., spans with the largest length and can be useful for monitoring bridge structures.

Keywords

cantilever bridges, rheological effects, concrete structures, mathematical modelling, service life, stress analysis

1 Introduction

Cantilever concreting technology in bridges was first used in 1951 by U. Finsterwalder during the building of a bridge over the Lahn Bulduinstein River. In those times, bridges constructed using this technology did not usually exceed half of the designed 100-year service life. Recently, several thousand bridges of this type have been made in the world. Cantilever concreting (or assembling) technology is one of the modern methods of constructing concrete bridges. Its main advantage is the savings made in materials, scaffolding costs and formwork, and above all, the possibility of building a span in many places at the same time. The latter, and especially the cyclicality of concreting individual segments, shortens the time of construction. Cantilever concreting technology in bridges is effective when a span length is between 50 m and 250 m.

The typical feature of bridges made using cantilever concreting technology is their external appearance [1], which is shown in Fig. 1. Their geometric characteristics are adapted to the adopted technology and load system in the construction phase [2]. In these types of long-span pre-stressed concrete bridges, the static scheme that occurs during the construction of the cantilevers has the main influence on the system of internal forces. Therefore, these bridges have a classically shaped structural system in the form of a girder with a box cross-section with a parabolically variable height.

A characteristic feature of many bridges, being objects of large spans made of pre-stressed concrete, are their excessive deflections [3–7]. An excessive deflection in the paper is assumed to occur when it exceeds the permissible value of the index ω = 1.25‰, which is calculated using the following formula:

$$\omega = \frac{w}{L}[‰], \tag{1}$$

where $w(t)$ [mm] is the displacement of the mid-point of the bridge span with length L [m]. According to the analyses given in [8], the main reason for the occurrence of excessive deflections is the structure's static scheme in the

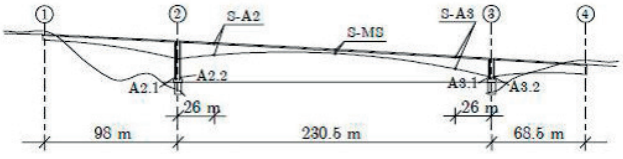

Fig. 1 Geometry and measuring system of the Norddalsfjord Bridge [3]

Cite this article as: Pisarek, B., Machelski, C. "Estimation of Rheological Effects in Cantilever Concrete Bridges on the Basis of a Span's Deflection Line", Periodica Polytechnica Civil Engineering, 66(1), pp. 228–234, 2022. https://doi.org/10.3311/PPci.18151

form of short spans that are adjacent to the main span, as can be seen in Fig. 1. Another reason is the technologies of constructing such bridges – usually a combination of different technologies.

The measurements of grade line changes of bridges spans made using the cantilever concreting method have been carried out for many years [9–11]. In the majority of these facilities there are no such operational problems as the ones that are considered in this paper. However, the phenomenon of large deflections that is analyzed in this paper is common, and until now not well investigated. A very good documented example of the analyzed problem is a bridge built in Norway [3]. The analysis concerns the Norddalsfjord Bridge, which is made of homogeneous concrete. In such bridges, lightweight concrete is used in their central part, as was the case in the Stølma Bridge, which has a record central span length of L = 301 m. Therefore, it can be considered as an example of a bridge construction that enables large spans to be achieved. In this bridge, eight years since the end of its construction, the deflection of w = 200 mm exceeded the design value. The underestimated deformability of the lightweight concrete [12, 11] was considered as the main reason for this deflection.

Fig. 2 shows a diagram of the increase in the Norddalsfjord Bridge's deflection [3]. The key of the diagram includes the time intervals between the reference measurement (0) 07.05.1987, and the analyzed measurements: (1) 05.06.1987, (2) - 27.03.2001 and (3) 16.10.2001. The difference in the results between measurements 2 and 3 can be treated as a seasonal change (spring/fall). In the time interval between measurement 0 and 2, i.e., after 14 years of operation, a significant value of the indicator was obtained.

$$\omega = \frac{166}{230.5} = 0.72[‰] \tag{2}$$

A negative example of the reduction of an excessive deflection can be seen in the Koror-Babeldoab Bridge [9, 13] with a center span of L = 231 m (x-axis in the Fig. 2. describe entire length of the bridge, side span [98 m + 68.5 m] as well as center span [230.5 m]). After 12 years of operation, the displacement in this bridge was equal to w = 1,200 mm, and therefore ω = 4.98‰. After 18 years, it increased to the value of w = 1,610 mm, which corresponds with ω = 6.68‰, and it exceeded the permissible value many times Eq. (1). Strengthening of the structure with the use of secondary post-tensioning did not work, and after a short period of operation ended in constructional failure.

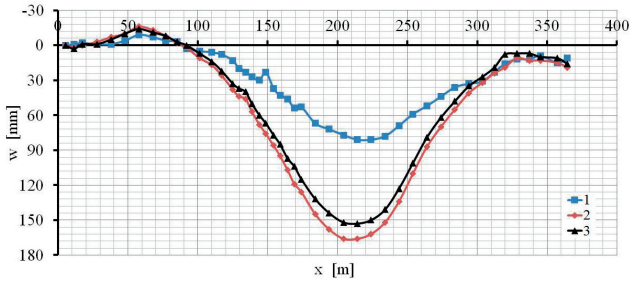

Fig. 2 The increase of deflections during the operation of the bridge [3]

2 Span deflections during the operation of a bridge

Although concrete creep tests have been carried out throughout the 20th century and are currently also being conducted, the problem of large deflections of pre-stressed concrete bridges is still not solved. The research shows that rheological processes do not tend to a finite value during the 100-year operation of a bridge. The phenomenon of large deflections is well known due to the monitoring of objects [11]. The purpose of this work is to determine the changes in internal forces that result from deflections as a function of time $\omega(t)$, which are obtained from measurements of bridges that are built using cantilever concreting technology.

The courses of the deflections of spans that were built using cantilever concreting technology can be considered in three time intervals [8]. In the initial period of several years after the completion of construction, the increments of deflections are by far the largest. In the first year, the progress of the deflection is the highest, and in the following years there is a slow stabilization. The second period involves the balanced increase of deflections. In turn, the third and the longest period of bridge operation (about 3/4 of service life), due to a lack of measurement data, can only be predicted [8].

The effect of the changes in a bridge's grade line in the form of measurements $r(x,tp)$ and $r(x,tk)$, which are obtained in two considered time periods $tp < \tau < tk$, are treated in the paper as a function of deflection.

$$w(x,t) = r(x,t_k) - r(x,t_p) \tag{3}$$

This deflection, without the participation of movable loads, is caused by the permanent loads of a bridge: the self-weight of the structure and equipment, as well as pre-stressing. Deflection of the span creates bending moments, as in dependence Eq. (4).

$$M(x,t) = E(t) \cdot I(x) \frac{d^2 w}{dx^2} = E(t) \cdot I(x) \cdot \kappa(x,t)\,. \tag{4}$$

The moment of inertia $I_x(x)$ is a function of time and depends on the geometry of the cross-section of the span and the position of the considered x point of the beam. During the operation of a bridge, there is a change in the deformation modulus of concrete $E(t)$. Both components form the stiffness of the bend span $EI_x(t,x)$. Therefore, if the assumption about homogeneity of concrete in segments is taken, the beam stiffness in Eq. (4) can be treated as one function. In the case of complex systems made of different concretes (ordinary and light), it is necessary to treat different sections of spans differently.

3 Curvature deflection functions

In Eq. (4) there is a second derivative of the deflection that results in the curvature of the beam in the considered point. Usually, the measurements of the grade line $r(x)$ are carried out using a regular grid of points that are distant from each other by the value c. Therefore, the curvature of the beam in point j can be obtained on the basis of deflections in adjacent points i and k, as in the differential equation [14].

$$\kappa_j = \frac{1}{c^2}\left(w_i - 2w_j + w_k\right) \tag{5}$$

In the case of $\kappa(x_j,t)$ taken from Eq. (4), the curvature is calculated in the analyzed point j. Therefore, the mathematical comparison of both values shows their convergence when the c-section tends to zero. However, in the case of measurements on an object, the differences in the value w in points i, j, k also tend to zero. Thus, in practice, the precision (accuracy) of measurements using geodetic techniques may be of great importance when selecting c.

Equation (5) assumes a regular arrangement of measuring points with a distance c between them. In the analyzed case of the Norddalsfjord Bridge, this situation did not occur. Therefore, in order to determine the deflection in the regular grid of points that are distant from each other by the value of c, it is recommended to use the computational scheme as in Fig. 3. In this scheme, the following was assumed: the position of the determined deflection value w_o at the beginning of the local coordinate system; distances; and also deflections of the measuring points i, j, k.A general formula is obtained from the second-degree parabolic approximation in the following form.

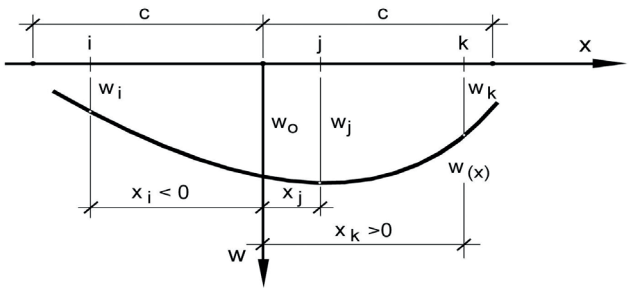

Fig. 3 Approximation of the deflection value

$$w_o = \frac{x_j \cdot x_k (x_k - x_j) w_i + x_i \cdot x_k \left(x_i - x_k\right) w_{jk}}{x_i^2\left(x_k - x_j\right) + x_j^2\left(x_i - x_k\right) + x_k^2\left(x_j - x_i\right)} + \frac{x_i \cdot x_j \left(x_j - x_i\right) w_k}{x_i^2\left(x_k - x_j\right) + x_j^2\left(x_i - x_k\right) + x_k^2\left(x_j - x_i\right)} \tag{6}$$

In the case of the deflection function as a second-order parabola, the same curvature is obtained at point j, as well as at the place of the created value w_o. Thus, by assuming the distances between points i–j as the value a, and between the j–k points as the value b, a general formula Eq. (5) is obtained in Eq. (7).

$$\kappa_0 = \kappa_j = \frac{2}{a \cdot b(a+b)}\left[b \cdot w_i - (a+b)w_j + a \cdot w_k\right] \tag{7}$$

In a special case, when $a = c$ and $b = c$, a regular arrangement of points and Eq. (5) are obtained.

The functions $\kappa(x,t)$, which are created on the basis of the functions $w(x,t)$ that are shown in Fig. 2, are presented in Fig. 4(a) and 4(b) and have a designation of basis in the key. The dependence Eq. (5) was used in the calculations. The value of the function curvature shows a very large dispersion of results and their irregular course. The basic reason for the irregular course of such diagrams is the limited accuracy of surveying measurements - 1 mm. For this reason, the direct use of the results of the measurements of the grade line in order to determine the bending moments using the relationship Eq. (4) has limited usefulness.

The curvature is determined from dependence Eq. (5) on the basis of the local deformation of the beam along Section 2c. From the form of solution Eq. (4), it is possible to analyze the section of the structure separated from the system. In the selected part of the deflection function there are no boundary conditions, e.g., the method of supporting the span or the type of load. Eq. (3) enables changes in the grade line to be analyzed in any chosen time intervals. Therefore, the condition of a structure can be analyzed from the reference measurement to any chosen measurement from Fig. 2. The deflection can also be treated as an effect that occurs between any measurements.

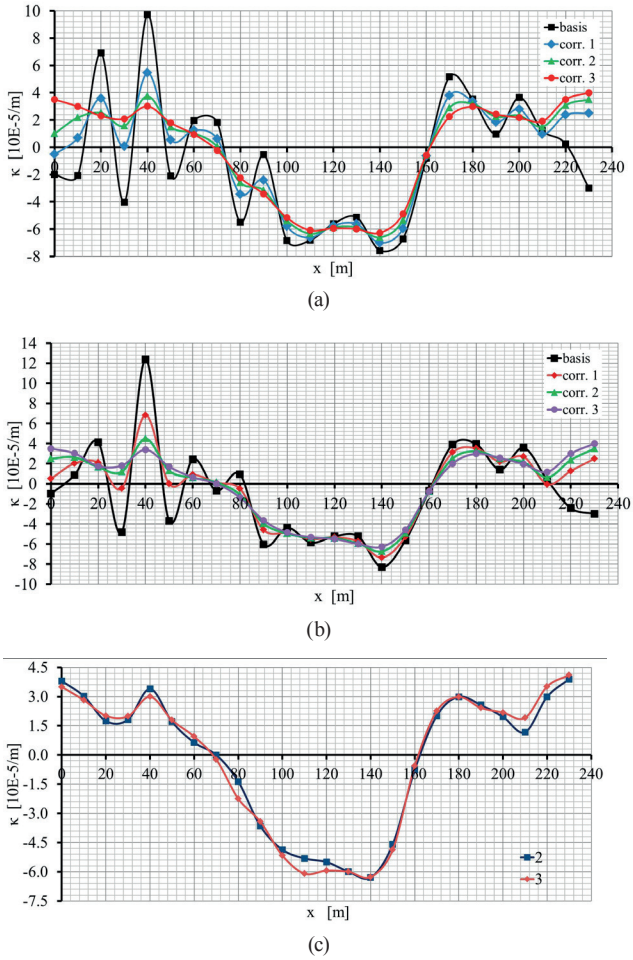

Fig. 4 Changes in the curvature of the span of the Norddalsfjord Bridge during the assessed time periods: a) measurement 2, b) measurement 3, c) comparison

4 Correction of the curvature determined from measurements

An algorithm of recalculating the deflection using the Mohr relationship, which is used in structural mechanics for modified bar systems, is proposed in the paper in order to improve (smooth out) the curve of function $\kappa(x,t)$.

$$w_j = \int_0^L \kappa(x,t) M_j(x) dx \tag{7}$$

In Eq. (8), the deflection of point j is calculated using the deflection function M_j that was formed from the bending moments resulting from the unit force in point j, which was determined in a convenient statically determined scheme, e.g., a simply supported beam. If the curvature had been calculated within the differential approach as in Eq. (4), the obtained value w_j would be identical to the initial one. Of course, this is the case when calculations are made using a uniform FEM model. A very important advantage of Eq. (8) is the elimination of the bending stiffness of a beam. Eq. (4) shows the complex dependence between the geometry of the structure and time.

In the case of using the curvature that is determined from the measurements and Eq. (4) in-stead of using the integral approach as in Eq. (8), it is convenient to use the matrix algorithm as in Eq. (9).

$$w_j = \frac{c}{6}\left(\boldsymbol{\kappa}^T \cdot \boldsymbol{B} \cdot \boldsymbol{m}_j\right) \tag{9}$$

In this approach, when the beam line is divided into a sequence of segments with length c, it is possible to create vectors $\boldsymbol{\kappa}^T$ and $\boldsymbol{m}_j$ from the curvatures and functions found in Eq. (8). These are the values of these functions at the beam measuring points. Assuming that the functions $\kappa(x,t)$ and $M_j(x)$ are continuous, you can use the form of matrix $\boldsymbol{B}$ in the calculations as in Eq. (10).

$$\boldsymbol{B} = \begin{bmatrix} . & . & & & \\ . & 4 & 1 & & \\ & 1 & 4 & 1 & \\ & & 1 & 4 & . \\ & & & . & . \end{bmatrix} \tag{10}$$

From Eq. (9), a slightly different value of deflection wj than from the measurements and Eq. (3) is obtained. This is due to the use of $\kappa(x,t)$, which is calculated as a differential approach with a form as in Eq. (5). In this case, the accuracy of the measurements of the grade line, as well as the deflections calculated using Eq. (3) as in Fig. 2, is of paramount importance.

The procedure that is presented in Eq. (9) can be repeated multiple times. In the first calculation, the measurement result (basis) is used, while in subsequent calculations (i), a new function $w(i)$ is used. In this way, the next curvature function $\kappa(i)$ is created. Therefore, this is a procedure of subsequent approximations. Fig. 4 shows the course of the smoothing of function $\kappa(x,t)$, which are marked in the key as corr. 1, 2, 3. The diagrams show a differentiated course of change in the curvature - sometimes even with a change in the value sign. Fig. 4(c) presents the curvature diagrams obtained after the third correction of the deflection function (the numbers of measurements are given in the key). In this case, almost consistent results were obtained despite considerable differences in the deflections that are given in Fig. 2. Visible deviations of the diagrams in two places: x = 110 m and x = 210 m can be treated as changes in the structure, e.g., due to post-tensioning or measurement inaccuracies. Differences in results were created in the short period of time between measurements in 2001 (from 27.03 to 16.10).

Fig. 5 presents the diagrams of deflection created in the process of smoothing the results that were obtained in measurements 2. In the case of the initial diagram basis, the deflection condition $w(L) = 0$ is not considered in the support point. The $w(x)$ function from the initial measurement should be corrected using orthogonal transformation so that $w(L) = 0$. In the corrected functions, the support condition results from the assumption of the form of the tracking function M_j from Eq. (8). An important element of the iterative process is the tracking of changes in the deflection function after subsequent shape adjustments. Small changes are visible in the diagrams given in Fig. 5.

It is important in the iteration process that the deflection functions do not differ significantly from the initial form that was obtained from the measurements. However, it is assumed that the measurement is carried out correctly and does not contain an erroneous reading. Further corrections of these diagrams may be inappropriate with regards to the description of the course of the phenomenon. The change in curvature does not have to be an absolutely smooth function, as is the case in a steel rolled beam that is loaded with a uniformly distributed force. Local disturbances of function $\kappa(x,t)$ can also be a result of changes in the structure of concrete, e.g., scratches or local slipping of cables.

5 Bending moments and stresses

In the situation when the geometry of the cross-section of the bridge is known, as in Fig. 6, the function of the moment of inertia $I(x)$ can be determined and the bending moments can then be calculated according to Eq. (11).

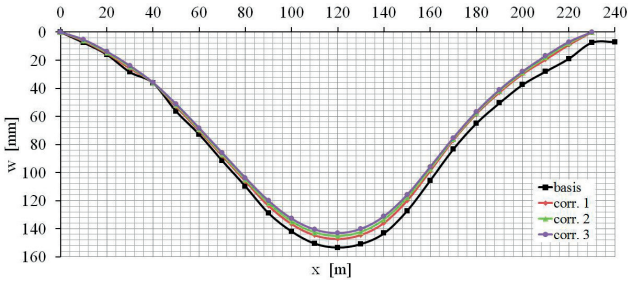

Fig. 5 Changes in the deflection of the Norddalsfjord Bridge span during the smoothing process from measurement 2

$$M(x) = E_t \cdot I(x) \cdot \kappa(x,t) \tag{11}$$

The moment function gives a view on the bending intensity over the span length, but its values are difficult to interpret. A better measure is the stresses that can be related to, e.g., the tensile strength of concrete. Therefore, based on the bending moment calculated in Eq. (11), more preferable is the stress function defined as

$$\sigma(x) = E_t \cdot v_j(x) \cdot \kappa(x,t)\,. \tag{12}$$

The distances of edges from the axis of inertia were designated as $v_j(x)$. Eq. (12) includes the product of beam curvature and Young's modulus of concrete.

Figs. 7 and 8 present the results obtained in the bridge shown in Fig. 6 in an analogical approach to the previously analyzed Norddalsfiord Bridge. The changes in the grade line of the bridge in Kędzierzyn-Koźle occurred within 76 months of operation, however, the measurement started after 30 months from the joining of cantilevers of the overhang span. The key of the diagram includes the

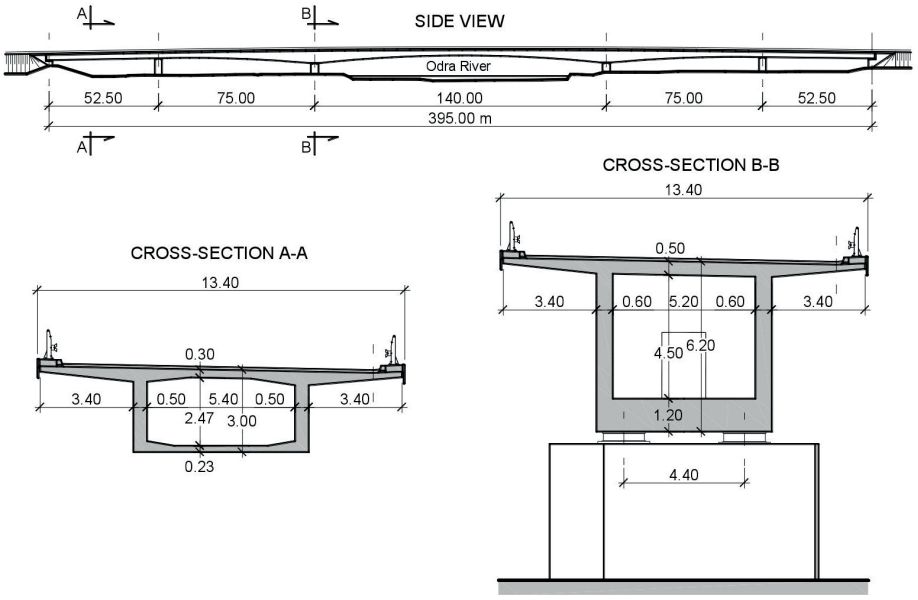

Fig. 6 Geometry of the Kędzierzyn-Koźle Bridge span

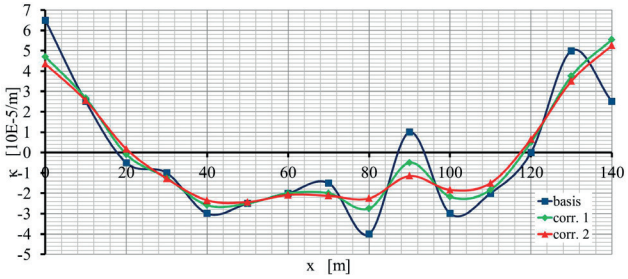

Fig. 7 Changes in curvature of the Kędzierzyn-Koźle Bridge span during the smoothing process

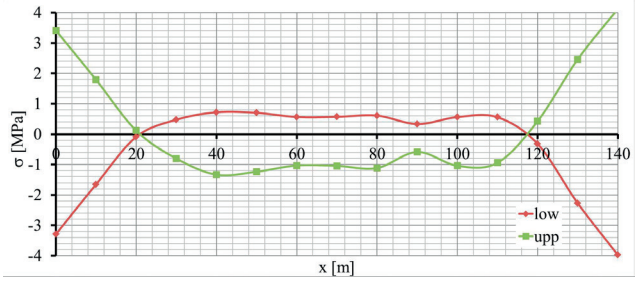

Fig. 8 Stresses on the lower and upper slab of the span of the bridge from Fig. 6

designation of the edge layers in the cross-section of the lower and upper slab. When interpreting stresses, it must be remembered that this applies to the situation when results of calculations are taken from the analyzed time interval. Therefore, it does not include the current state of the structure because the result of the calculations is not referred to the initial value - in the analyzed unknown situation. In the calculations, the value of E_t = 25,000 MN/m^2 was adopted without any additional justification (value assumed, based on the experience). The normal stresses showed in Fig 8. depend on the taken value of the E_t. This is due to the fact that the construction process, as well as the actual state of concrete effort, are not taken into account.

In the diagrams in Fig. 8, there are higher stress values in the support zones (-10 < x < 15 and 125 < x < 150 m) than in the span. This is due to the adoption of the beam computational model. The comparison of curvatures Fig. 7 and stresses Fig. 8 shows a reduction that results from the moments of inertia.

In the case of estimating the difference in the unit deformations, the stiffness of the girder is neglected - it is variable in time due to concrete creep. Therefore, from Eq. (11), the following simple relation is obtained

$$\Delta\varepsilon = \varepsilon_{low} - \varepsilon_{upp} = h(x)\cdot\kappa(x,t)\,, \tag{13}$$

where $h(x)$ is the distance of the analyzed measuring points of the lower and upper slab. The three cross-sections shown in Fig. 1 were analyzed in the evaluated bridge. The span height was equal to 13 m above the support and 3 m in the middle of the span. Based on the calculations and diagrams given in Fig. 3, the following were estimated:

- the cross-section in the middle - S-MS when h = 3 m.

$$\Delta\varepsilon = 3.0\cdot 6.0\cdot 10^{-5} = 180\cdot 10^{-6} \tag{14}$$

- the cross-section above the supports - S-A2 and S-A3 when h = 9 m.

$$\Delta\varepsilon = 9.0\cdot 1.8\cdot 10^{-5} = 162\cdot 10^{-6} \tag{15}$$

These values are similar to those obtained during the measurements and those from special computational models in [3].

6 Conclusions

A characteristic feature of bridges as large span objects made using cantilever concreting technology is the formation of excessive deflections ($w > L/800$, value estimated, based on the experience from polish bridges) which result from the rheological processes occurring in concrete and pre-stressing steel [15]. Moreover, deflections in these objects may be a result of material destruction, such as cracks or a change in the construction's load scheme, e.g., subsidence of supports. The total effect of exploitation is the changes in the bridge's grade line that are observed on site in the results of the conducted surveying measurements. The difference in grade lines between two selected observation times (measurements) is treated in the paper as the deflection line of the span. Span deformation occurs together with a change in internal forces and support reactions [16].

The paper presents the analysis of examples of bridges for which the measurement results of the span's grade line were available in literature. Therefore, in order to draw general conclusions about the problem analyzed in the paper, a larger group of objects is necessary, as is the case in [9].

The characteristic functions of the span deflection result from the geodetic measurements [17]. Due to the accuracy of geodetic measurements, it is not possible to calculate the internal forces using derivatives of function $w(x)$ from the deflection diagrams. The paper proposes an algorithm for the correction of the deflection function. It is characterized by a significant improvement of the calculation results and, to a small extent, leads to the smoothing of the original measurement results. The algorithm is adapted to the analysis of the selected section of the structure, e.g., a span with the largest length that is built using cantilever concreting technology. The advantage of the algorithm is the ability to analyze a structure in any chosen time period

(between two considered measurements). The results of such analyses are not related to the initial state, e.g., the moment of joining the structure. The advantage of this algorithm is the elimination of the geometrical characteristics of the transverse cross-section of a span.

A separate issue in concrete cantilever bridges is the construction phase. Its feature is the large dispersion of measurement results of deflection, which is caused by many factors with random characteristics, such as: construction technology, construction time, concreting time, climate, concrete strength, used aggregate, reinforcement grade, pre-stressing ratio, and the most important rheological processes [11, 18]. Therefore, calculations for the construction phase must be conducted separately.

References

[1] Matsuyoshi, H., Duc Hai, N., Kasuga, A. "Recent technology of prestressed concrete bridges in Japan", [pdf] In: IABSE-JSCE Joint Conference on Advances in Bridge Engineering-II, Dhaka, Bangladesh, 2010, pp. 46–55. Available at: http://iabse-bd.org/old/43.pdf

[2] Ghali, A., Elbadry, M. "Deformations of Bridge Structures: Analysis Techniques and Calibration by Measurements on the Confederation Bridge Canada", presented at Bridge Engineering Conference, Sharm El Sheikh, Egypt, March, 26–30, 2000. [online] Available at: https://www.researchgate.net/publication/261367167

[3] Bažant, Z. P., Hubler, M. H., Yu, G. "Excessive Creep Deflections: An Awakening", [pdf] Concrete International, 8(33), pp. 44–46, 2011. Available at: https://citeseerx.ist.psu.edu/viewdoc/download?doi=10.1.1.471.4734&rep=rep1&type=pdf

[4] Kalný, M., Souček, P., Kvasnička, V. "Long-term behaviour of balanced cantilever bridges", presented at ACEB Workshop: Innovative Materials and Tecniques in Conference Construction, Corfu, Greece, Oct. 10–12, 2010.

[5] Keijer, U. "Long-term Deflections of Cantilever pre-stressed Concrete Bridges", In: IABSE Symposium, Design of Concrete Structures for Creep, Shrinkage and Temperature Changes, Madrid, Spain, 1970, pp. 27–34. http://doi.org/10.5169/seals-6904

[6] Machelski, C., Pisarek, B. "Change of the grade line of bridges constructed with cantilever concreting technology", Architecture, Civil Engineering, Environment, 11(2), pp. 65–72, 2017. https://doi.org/10.21307/ACEE-2018-023

[7] Trost, H. "Zur Berechnung von Stahlverbundträgern im Gebrauchszustand auf Grund neuerer Erkenntnisse des viskoelastischen Verhaltens des Betons" (About the calculation of steel composite girder in the operational time on the basis to the recent findings of the elastoviscous behavior of concrete), Der Stahlbau, 11, pp. 321–331, 1968. [in German]

[8] Machelski, C., Pisarek, B. "Analysis of deflection line in the bridge superstructures constructed using cantilever concreting method", presented at fib Symposium, Krakow, Poland, May, 27–29, 2019.

[9] Bažant, Z. P., Li, G.-H., Yu, Q., Klein, G., Kristek, V. "Explanation of Excessive Long-Time Deflections of Collapsed Record-Span Box Girder Bridge in Palau. Preliminary report", presented at the 8th International Conference on Creep and Shrinkage of Concrete, Ise-Shima, Japan, March, 9, 2008.

[10] Křístek, V., Bažant, Z. P., Zich, M., Kohoutková, A. "Box Girder Bridge Deflections", ACI Concrete International, 28(1), pp. 55–63, 2006. [online] Available at: https://www.researchgate.net/publication/285638399

[11] Takács, P. F. "Deflections in Concrete Cantilever Bridges: Observation and Theoretical Modelling", [pdf] Doctoral Thesis, Norwegian University of Science and Technology, 2002. Available at: https://ntnuopen.ntnu.no/ntnu-xmlui/bitstream/handle/11250/231135/121731_FULLTEXT01.pdf?sequence=1&isAllowed=y

[12] Bacinskas, D., Rumsys, D., Sokolov, A., Kaklauskas, G. "Deformation Analysis of Reinforced Beams Made of Lightweight Aggregate Concrete", Materials, 13(1), Article number: 20, 2020. https://doi.org/10.3390/ma13010020

[13] Tang, M.-C. "The Story of the Koror Bridge", International Association for Bridge and Structural Engineering (IABSE), Zurich, Switzerland, 2014. https://doi.org/10.2749/cs001

[14] Pisarek, B. "Analyse of the grade line and the rheological effects in the bridges constructed with cantilever method", In: 6th Young Engineering Colloquium, Berlin, Germany, 2019, pp. 66–68.

[15] Dolinajová, K., Moravčik, M. "Monitoring and Numerical Analysis of Construction Stages on the Bridge Realized by the Free Cantilever Method", Procedia Engineering, 65, pp. 321–326, 2013. https://doi.org/10.1016/j.proeng.2013.09.049

[16] Tassi, G., Rózsa, P. "Forces in prestressed concrete bridges constructed cantilevering", Periodica Polytechnica Civil Engineering, 36(3), pp. 355–361, 1992. [online] Available at: https://pp.bme.hu/ci/article/view/3853

[17] Burdet, O., Badoux, M. "Deflection monitoring of pre-stressed concrete bridges retrofitted by external post-tensioning", [pdf] In: IABSSE Symposium, Rio de Janeiro, Brazil, 1999, pp. 396–403. Available at: http://citeseerx.ist.psu.edu/viewdoc/download? doi=10.1.1.548.2890&rep=rep1&type=pdf

[18] Rüsch, H., Jungwirth, D. "Stahlbeton-Spannbeton Band 2: Berücksichtigung der Einflüsse von Kriechen und Schwinden auf das Verhalten der Tragwerke" (Reinforced Concrete-Prestressed Concrete, Volume 2, Accounting for the Effects of Creep and Shrinkage on the Behavior of Structural Systems), Werner Verlag, Berlin, Germany, 1976. [in German]